



Evaluation of Digital Surface Model Data to Improve Forest Biomass Estimation from SPOT HRG

Myint Hlaing

Arbetsrapport 293 2010
Master 30hp D
MSc in European Forestry

Handledare:
Jörgen Wallerman

Sveriges lantbruksuniversitet
Institutionen för skoglig resurshushållning
901 83 UMEÅ
www.srh.slu.se
Tfn: 090-786 81 00



ISSN 1401-1204
ISRN SLU-SRG-AR-293-SE

Evaluation of Digital Surface Model Data to Improve Forest Biomass Estimation from SPOT HRG

Myint Hlaing

Thesis submitted in a partial fulfillment of the requirement for the Degree of Master of Science in
European Forestry

Master thesis in Forest Management

MSc in European Forestry

EX0599

Supervisor: Jörgen Wallerman, SLU, Department of Forest resource management, Section of Forest Remote Sensing

Examiner: Håkan Olsson, SLU, Department of Forest resource management, Section of Forest Remote Sensing

Sveriges lantbruksuniversitet
Institutionen för skoglig resurshushållning
Utgivningsort: Umeå
Utgivningsår: 2010

ISSN 1401-1204
ISRN SLU-SRG-AR-293-SE

Summary

Remote sensing techniques play a crucial role to upscale aboveground biomass estimates from local, regional to global scale. The objective of the present research was to use previously not evaluated canopy height model (CHM) data to enhance aboveground biomass estimation from SPOT HRG imagery (HRG). The different CHMs data evaluated were digital surface models mapped using photogrammetric processing of data acquired by the airborne Digital Mapping Camera from Zeiss/Intergraph (DMC), SPOT High Resolution Stereo (HRS) and Airborne Laser Scanning (ALS) data. The pixel sizes range from one half meter to twenty meter. The study site is the watershed of the Krycklan stream located in the North Eastern part of Sweden (Lat. 64°14' N, Long. 19°50' E). The study area covers approximately 7800 hectares and is characterized by boreal forest dominated by Norway spruce (*Picea abies*) and Scots pine (*Pinus sylvestris*).

The remotely sensed data derived spectral bands and canopy heights (CHMs) were used to fit regression models and to perform cross validation at plot level to estimate aboveground biomass. The resulting models were used to produce raster maps. Furthermore, accuracy assessment in terms of root mean square error (RMSE) of stand level estimations was computed based on an independent field measured dataset.

The adjusted R^2 for stand level estimates of above ground tree biomass was 60% and the RMSE was 31.8% when using SPOT HRG alone. The corresponding values of CHM data were 23.0% R^2 (adj) and 35.4% RMSE for SPOT HRS; 77% R^2 (adj) and 18.8% RMSE for Z/I DMC; and 80.7% R^2 (adj) and 20.2% RMSE for ALS respectively. The results of cross validation of all models comply with the standard limit falling between 1.04 and 1.15. The former corresponds to a model with one explanatory variable and the latter was for 5 or 6 explanatory variables.

Fusing the data sources of HRG and CHM improved aboveground biomass prediction in terms of both R^2 and RMSE for all sensors data. For HRS, R^2 improved from 23.0% to 50.2% and RMSE improved from 35.4% to 26.9%. R^2 of Z/I DMC increased from 77.0% to 80.0% and RMSE improved from 18.8% to 16.9%. ALS derived canopy height measurements without vegetation ratio increased R^2 from 80.0% to 84.5% and RMSE improved from 20.2% to 15.6%. Using ALS data including vegetation ratio decreased R^2 from 90.5 % to 90.2% but RMSE improved from 15.7% to 14.1%. HRS and DMC increased the coefficient of determination and improved mapping accuracy when combined with the multi-spectral bands from HRG. ALS derived measurements had much higher R^2 and accuracy when the canopy height was combined with vegetation ratio in estimating aboveground biomass. The use of digital CHM do appear promising to estimate dry biomass content and monitor carbon uptake for many important future applications.

Keywords: aboveground biomass, digital surface models, remote sensing, prediction, mapping accuracy.

Contents

Summary	2
1. Introduction	4
2. Materials and Methods	8
2.1 Study Site	8
2.2 Data Acquisition.....	10
2.3. Image Processing and Data Extraction.....	12
2.4. Data Analysis	13
3. Results	15
3.1. SPOT HRG.....	15
3.2. SPOT HRS	16
3.3. Z/I DMC.....	17
3.4. ALS (Canopy Height Model).....	18
3.5. SPOT HRS and SPOT HRG	20
3.6. Z/I DMC and SPOT HRG.....	21
3.7. ALS (Canopy Height Model) and SPOT HRG	22
3.8. ALS (Canopy Height Model and Vegetation Ratio).....	24
3.9. ALS (Canopy Height Model and Vegetation Ratio) and SPOT HRG	25
4. Discussion and Conclusions.....	31
Acknowledgements	34
References	35

1. Introduction

Biomass estimation has been undertaken through the various approaches that encompass using the allometric equations from field measurement, remotely sensed techniques and modeling with GIS depending on the scale and in the context of spatial and aspatial conditions. The commonly used term biomass is the total amount of aboveground living organic matter in trees expressed as oven-dry tons per unit area (FAO, 1997). Biomass estimation plays a crucial role in a broad range of applications such as accounting the carbon budget for various climate reporting tasks, estimating forest productivity, modeling energy resources, and characterizing the forest conditions and processes (Wulder et al, 2008). The presence and changes of biomass is closely related to the carbon emission, which in turn affects terrestrial ecosystem functions and climate change, to name a few fundamental processes. Accurate biomass mapping from local to global scale is becoming important for reducing the uncertainties of carbon sequestration cycles and achieving insight of its influence on soil and land degradation and ecological stability (Foody, 2003). To reduce costs and cover large areas with relatively high accuracy, remote sensing techniques is promising and has a large potential role in forest management planning and monitoring. Besides, it is the fact that constraints in direct field measurement and GIS based modeling using ancillary data can often be overcome by remote sensing techniques. For instance, labor intensive, difficult implementation in remote areas and higher cost in field measurement methods and the unavailability of good ancillary data in GIS are limiting factors for estimation. Thus, all these factors are of keen interest for scientific researchers to apply remote sensing in a wide range of environmental applications. Biomass estimation by remote sensing techniques has been documented by many researches. However there are still many challenges remained especially in the diverse stand structure with complex biophysical environments (Dengsheng, 2005). In addition, the application of currently used 2D techniques, for instance, from optical imagery and radar data, has a limited capacity to estimate high biomass. Thus 3D techniques need to be developed to fill up this gap.

Biomass is the dry mass of live plant materials in the forest ecosystem. Aboveground (ABG) biomass includes wood stem, branches, foliages, bark, litters and dead leaves while belowground biomass constitutes of the roots and stump. Aboveground biomass stands approximately for 78% and 22% represents for belowground biomass in boreal biome forest. Being difficult to administer field measurement data for belowground biomass, most of the researches dealt with aboveground woody biomass content (Dengsheng, 2006). Forestry management and Planning in Sweden, where covered with 23 millions of forest land, have been carried out on the basis of 3 level needs; which are (i) the needs of authorities to overview all forest owners; (ii) More detailed information of each forest estate for individual forest owners; and (iii) timely accurate information for on-going and already harvested area for individual forest stands (Olsson et al, 2005). The use of various spaceborne and airborne sensors along with the aerial photo interpretations in Sweden have provided such data for stem volume estimation at stand level (Table 1, reproduced from Magnusson (2006)). The use of small foot print ALS data provided the highest accuracy (12%) in terms of root mean square error followed by the data integration method of CARABAS radar data and SPOT satellite data (16%).

Biomass plays a crucial role for bio-energy use and carbon flux report in line with the guidelines of Kyoto Protocol and UNFCCC. The forest biomass can replace the fossil fuel use which is a threat for global climate change by releasing green house gases into the

atmosphere. Even though numerous researches were carried out monitoring on forest biomass estimation with the special emphasis on the use of various remotely sensed data, the accuracy assessment derived from different sensors at different levels varied.

Table1. Stem volume estimation accuracy on stand level for different remote sensing sensors, validated at the same test site; all estimates except the photointerpretations measurements are made with regression technique at semiboreal forest in southern Sweden

Sensor or sensors used	Reference	RMSE(%)
SPOT HRVIR, SPOT HRG, Landsat ETM+ satellite data	Fransson et al 2004	23-31
Interpretation of aerial photos	Magnusson and Fransson 2005	18-24
CARABAS VHF SAR	Magnusson and Fransson 2004	19
Combination of CARABAS and SPOT HRVIR	Magnusson and Fransson 2004	16
Laser Scanner	Fransson et al 2004	12

Source Magnusson (2006) Doctoral Thesis, ISSN 1652-6880, SLU, Umeå

According to the Intergovernmental Panel on Climate Change (2004), the estimation of woody forest biomass and carbon sink, in general, lack degree of certainty in local, regional and global dimensions. Some of the recent research findings that had used both passive and active sensors regarding with aboveground biomass estimations were varied from region to region with respect to the use of spatial, temporal and spectral resolutions.

Regarding the use of ALS data, Holmgren (2003) applied regression models to predict forest volume and tree height in southern part of Sweden by using small foot print laser scanning data. The results at 10 m radius plot level were ($R^2 = 90\%$) and (RMSE = 22%) for stem volume estimation by using laser derived mean height and crown coverage area as predictors, meanwhile RMSE for stem volume was 26% when tree heights in conjunction with stem numbers were used. Naesset (2008) reported the coefficient of determinations of the aboveground biomass being 88% and belowground biomass 85% through the use of small foot print airborne laser scanner alone with average pulse intensity 1.1 per square meter. This research was carried out in boreal forest in South Norway by using regression analysis. Accuracy was 21% and 22% RMSE for aboveground and belowground biomass predictions, respectively. Another research done by Nasset (2007) predicted 6 biophysical properties in boreal forest in Norway by using small footprint 0.8 pulse per meter square laser scanner data. Main biophysical variables predicted were mean and dominant heights, basal areas and volumes. The content of aboveground forest biomass was estimated in the Eastern part of a forested area in Canada with the use of ALS based biomass equation that resulted in a R^2 of 65% ($n = 207$) at plot level. Distributional parameters from small footprint discrete return ALS was applied to estimate aboveground forest biomass in unmanaged forest in Mediterranean zone in Spain based on tree height, intensity and the combination of height and intensity. The estimation of species specific models by using distributional parameters in Spain resulted in a R^2 greater than 85% for black pine, 70% for Spanish Juniper and 90% for Holm oak (Garcia et al, 2010). The small footprint ALS data was applied for single tree based algorithm to predict the aboveground biomass by (Zachary J.B and Randolph H.W 2005) in central Virginia, USA. They found that root

mean square error corresponding to diameter at breast height threshold greater than 7cm and 10cm were 14.2% and 14.8% with variation of R^2 of 0.50 and 0.53 respectively.

Using optical data of boreal forest, Hall et. al (2006) modeled aboveground biomass and volume as functions of tree height and crown closure at the plot level, which were later aggregated to stand level in boreal forest. In his research the spectral bands from Landsat ETM+ were applied to model the aboveground biomass and volume by using height and crown closure in the boreal forest in west central Alberta, Canada. The direct estimation of aboveground biomass from Landsat ETM+ spectral bands resulted in an adjusted $R^2 = 0.40$ and $RMSE = 57.2$ ton per hectare and volume estimates with an adjusted $R^2 = 0.30$; and $RMSE = 110.8m^3$ per hectare. Depending on the use of pixel size (from fine to coarse resolution) and vegetation indices (for example NDVI, LAI), the aboveground biomass estimates and accuracy varied. For instance, the application of Quickbird HRSI imagery (2.4 m pixel size) to predict the aboveground biomass relative to shadow fraction in black Spruce dominated boreal forest in Canada by Leboeuf et al (2007) showed R^2 (0.85- 0.87) and $RMSE$ (14.2 ton/ha). Aboveground forest biomass was estimated by using Landsat ETM+ medium pixel size in tropical, temperate and boreal forest as in (Lu, 2004, Zheng, 2004, Hall 2006) Aboveground biomass estimated by using visible to shortwave infrared advanced spaceborne thermal emission and reflection radiometer (ASTER) data in Finland was reported as the lowest $RMSE$ at 41% (Heiskanen, 2006).

Data integration methods using different sensors, spectral, spatial and temporal combinations have been developed (Gong 1994, Pohl and Van Genderen 1998, Chen and Stow 2003). In estimating aboveground woody biomass, Popescu et al (2004) integrated small footprint ALS data and multispectral data from NASA's Airborne Terrestrial Land Applications Scanner (ATLAS) for estimations of biomass in deciduous and pine stands in the southeastern USA, using small scale plot level and individual tree measurements. The coefficient of determination, R^2 , for biomass models were 0.32 for deciduous and 0.82 for pine trees. It was found that the use of data fusion of ALS and optical imagery improved biomass and volume estimation as compared to the use of ALS data alone. The combination of ALS, Synthetic Aperture Radar and Interferometry SAR (InSAR) was more successful to predict aboveground biomass of stands with open pine forests in Southwestern USA, compared to using only InSAR data (Hyde et al, 2007). There, canopy height from ALS data alone explained 83% of the biomass variability and cross sectional return of GeoSAR P band GeoSAR/InSAR canopy height explained 30% of the biomass variability. Integration of ALS and Radar measurement improved somewhat, R^2 improved from 83% to 84 %, and prediction error was reduced from 26 ton/ha to 24.9 ton/ha.

Accuracy of volume and biomass estimations using only spectral information from 2D imagery obtained with optical sensors is limited, especially for high biomasses (Patenaude et al, 2005). One way to add additional relevant data to improve biomass estimation is to use digital Canopy Height Models (CHM) acquired from a digital surface model (DSM) of a canopy roof. CHMs can be acquired by subtracting a high quality Digital Elevation Model (DEM) derived from ALS data. Hence, given an accurate ALS terrain model it is possible to extract data about the vegetation height above ground in the form of CHMs. Today, there are several new possibilities arising to utilize DSM data from already currently operating sensors. This is mainly governed by the increasing availability of

accurate DEMs acquired by ALS surveys. This study is focused on two such DSM data sources, the HRS sensor onboard the space-borne SPOT 5 satellite, and photogrammetric modeling of the standard imagery acquired by the DMC camera at the regular aerial photography mapping of Sweden by the Swedish National Land Survey (www.lantmateriet.se). In detail, this research addresses the possibility to enhance biomass prediction by using SPOT HRG data in combination with CHM information. Mapping using this technique applied on CHM data from HRS or DMC has, to our knowledge, not been reported yet in any research paper. Here, CHMs derived from DMC and HRS were evaluated in combination with SPOT HRG data. Furthermore, models utilizing CHM and vegetation density variables derived from ALS as well as SPOT HRG data was also evaluated here, to serve as base-line references of known prediction performance. Multiple regression analysis was applied to utilize extracted image features to predict aboveground biomass (b) at plot level, and to also evaluate prediction accuracy at forest stand level using an independent evaluation dataset. Prediction using the multispectral bands response of HRG was designed as a benchmark in this research framework. The data integration methods between HRG and each of CHM were evaluated so that the comparisons were examined for accuracy assessments of each data fusion method as well as single sensor use method.

The aim of the current study was to evaluate and compare the biomass mapping performance of seven different models (combinations of sensor data);

1. SPOT HRG only, using the response from spectral bands, band ratios, and band combinations,
2. SPOT HRS only, i.e. CHM data from the HRS sensor,
3. ALS data only (CHM and Vegetation ratio),
4. DMC only (CHM from DMC sensor)
5. SPOT HRG and CHM data from HRS,
6. SPOT HRG and CHM data from DMC,
7. SPOT HRG and CHM data from ALS.

2. Materials and Methods

2.1 Study Site

This work was performed at the Krycklan watershed area (Lat. 64°14' N and Long. 19°40' E), covering approximately 6800 ha, located north east of Umeå city in Västerbotten County. The area consists of boreal forest dominated by Scots pine (*Pinus sylvestris*), Norway spruce (*Picea abies*), and Birch (*Betula spp.*). Coniferous species represent more than 80% of the forested area. The dominant soil type is till soil, a mixture of sandy coarse and mineral soil type (Krantz, 2009). Elevation above sea level ranges from 160 to 400 m above mean sea level. The mean forest stem volume is 151.5 m³/ha, and ranges to a maximum of 375m³/ha. Mean tree height is 14.6 m and maximum 23.1 m.

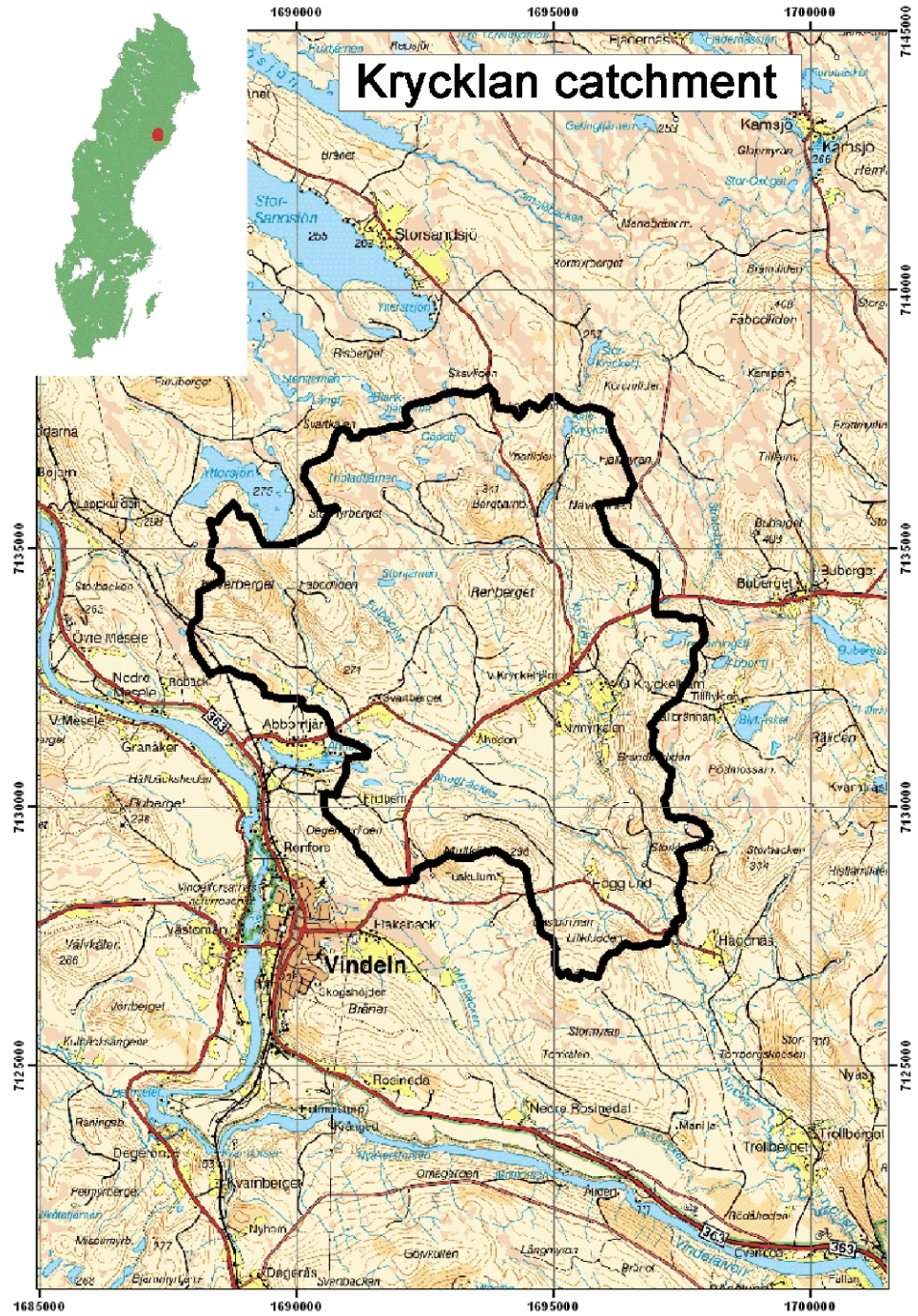


Figure 1. Map of the Krycklan study area. © Lantmäteriverket.

2.2 Data Acquisition

One hundred and nine georeferenced field measured sample plots had been objectively measured in 2007 throughout the entire Krycklan watershed area based on a systematic sampling design (Table 2). At each plot, all trees within 10 m radius were callipered and additional measures were made at a sub-sample of those trees. Furthermore, additional field survey was conducted year 2008 for 31 forest stands (2.4-26.3 ha). In total, 311 circular sample plots were systematically sampled within the 31 forest stands. This dataset was used as an independent dataset to assess stand-level prediction accuracy (Table 3). In each forest stand, 8 to 13 circular plots had been surveyed with a systematic spacing of 50 to 160 meters depending on the size of stand. The spacing in each forest stand was designed to obtain on average 10 plots per stand. All trees with a DBH (diameter at breast height) > 4 cm were callipered and the species were registered within each 10 meter radius sample plot. Sample trees were randomly selected with probability proportional to basal area, and measured to determine height and age. Site variables such as site index, vegetation type, soil type, previous silvicultural treatments (for instance, thinning) were recorded for each plot. The aboveground biomass was computed using the functions of Petersson (1999).

Table 2. Characteristics of the 109 field plots used for model development

Variables	Min	Max	Mean	STDV
Tree Height (m)	8.51	23.1	14.6	3.16
Tree Diameter (cm)	8.35	36.25	16	4.59
Volume (m ³ /ha)	20.04	374.25	151.5	81.4
ABG Biomass (ton/ha)	10.07	196.83	80	39.82

Table 3. Characteristics of the 311 field plots used for evaluation

Variables	Min	Max	Mean	STDV
Tree Height (m)	5.48	31.9	16.2	5
Tree Diameter (cm)	3.2	50.9	12.7	7.5
Volume (m ³ /ha)	0.42	644.8	171.8	100.3
ABG Biomass (ton/ha)	0.32	294.1	88.1	46.3

The forest stand map of the study area was produced using manual interpretation of aerial photos in a digital photogrammetric station (Åge, 1985). This was performed using scanned analogue images covering most of the area, and new DMC images which were available only for the eastern part of Krycklan. Figure 2 shows HRG imagery, the outlines of the 31 forest stands, and the field measured plots. These field measured plots were used to compute cross validation in order to assess stand level prediction accuracy.

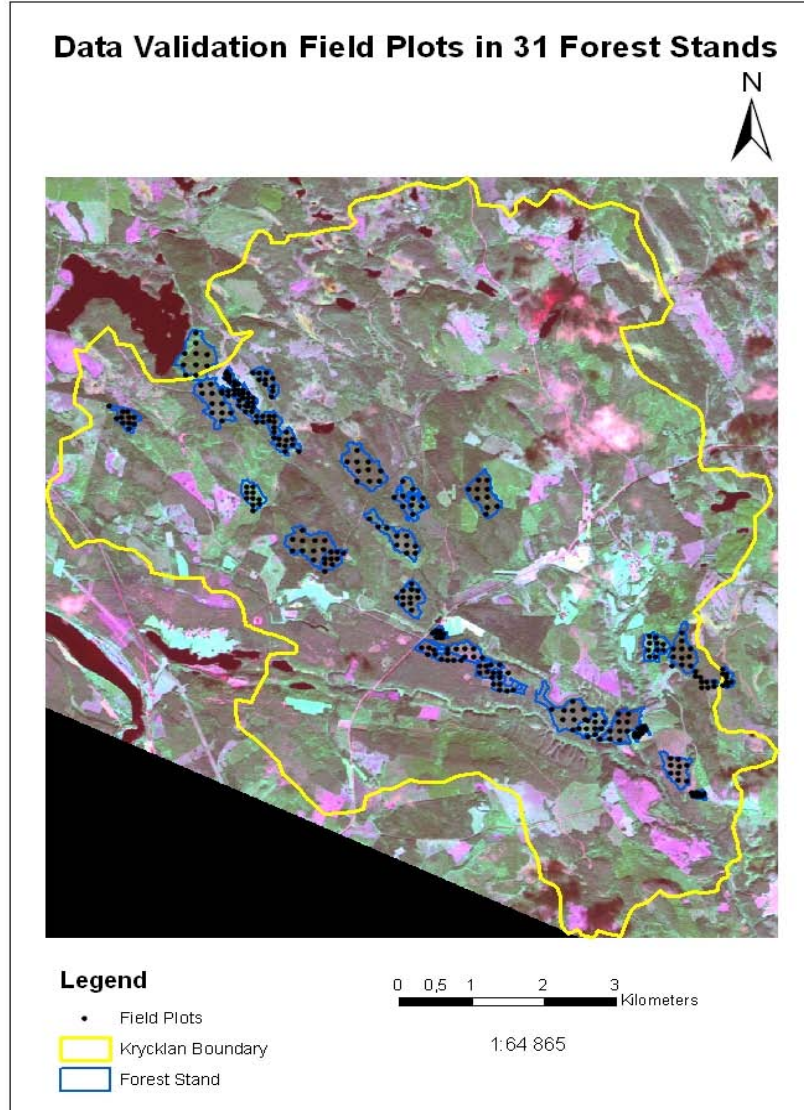


Figure 2. Evaluation forest stands and HRG used in the Krycklan watershed study area.

A multispectral SPOT HRG image, geometrically precision corrected and projected into Swedish National Grid (RT 90), was used. This image includes 4 bands; green (0.49-0.60 μm), red (0.61-0.68 μm), Near IR (0.78-0.89 μm) and shortwave IR (1.58-1.7 μm .) respectively with 10m pixel size for the first three bands and 20 m pixel size for the SWIR band. The image was acquired on 31th August 2008. Four spectral bands (green, red, near infrared, and shortwave infrared), band squares, the ratio of bands were the key variables applied for the data analysis. The imaging swath width is 60x60 km, the viewing angle 22.5°, and 8 bit radiometric resolution. The altitude of orbital path is about 822 km and 98.7 degree sun-synchronous.

The High Resolution Stereoscopic instrument (HRS) has been designed to produce digital elevation model data. HRS consists of two telescopes that allow along-track stereoscopy with a 20° fore view and a 20° aft view (Bouillon, 2006). Thus, a Digital Elevation Model (DEM) can be generated from the HRS image data. The canopy height obtained from HRS was used for model formulation at raster level and computation of RMSE. HRS data was acquired on 18th March 2005 and 31st July 2005 to compensate the cloud cover area between two dated imageries that brings up cloud free whole study area.

The National Land Survey (NLS) in Sweden acquired their first digital camera (Z/I DMC) in 2004. This camera registers blue, green, red and near-infrared and panchromatic wavelengths. Resolutions of the sensors are 2048 x 3072 pixels in the multispectral bands and 7,680 x 13,824 pixels for the panchromatic band (Intergraph, 2010). The wavelengths composed are blue (400-580 nm), green (500-650 nm), red (590-675 nm), and NIR (675-850 nm), respectively. Since 2005, one third of the Sweden is planned to be annually photographed using DMC at a standard flight altitude of 4800 m. The standard digital mapping photos are produced by 60% stereo overlap along the flight track and 30% overlap between the adjacent tracks. This results in high resolution (pixel size 0.5 m) multispectral image data. DMC images used in this study were acquired by NLS during the vegetation season in 2009 at the standard altitude and standard stereo overlap. Using the image data, a DSM was generated by NLS using photogrammetric modeling in the softwares Match T and Match AT (www.inpho.com). The canopy height, its logarithm form, and square of canopy heights were applied for data analysis.

Airborne Laser Scanning (ALS) provides three dimensional measurements of ground level, canopy height and structure. One important feature of ALS is that the laser beams can penetrate the vegetation and makes it possible to generate Digital Elevation Models (DEM) and Canopy Height Models (CHM) with high precision. Mapping forest using ALS consists mainly of two approaches- the area based approach and the single tree detection approach. The single tree approach require high pulse density ($> 5/m^2$) meanwhile the area based approach is feasible using low pulse density (about $1/m^2$). The data from the TopEye airborne laser scanner was used in this study, data with 4-5 pulses per m^2 with complete cover of the Krycklan study area. The ALS data were acquired in August 2008 and were used to render different percentile height values and vegetation ratio for the study area. Various percentile heights (CHM), vegetation ratio, and logarithm transformations of these heights were used in the data analysis.

2.3. Image Processing and Data Extraction

The ALS data had been classified as ground hits or non-ground hits by using the standard algorithm in the TerraScan software; a rectangular grid had been created over the cloud points. For each cell, the lowest point was chosen as a connection point (ground hit) which was then used to construct the ground surface by a triangulated irregular network (TIN). Then, an iterative process of accepting or rejecting a point as a possible ground hit was undertaken by adding one new point at a time using different criteria as distance between the new point and the present TIN or angle to the TIN with and without the candidate points. Using the resulting TIN, a DEM of the ground height above mean sea level was made. The returned signals from the vegetation are used to determine the vegetation canopy height by calculating the vertical distance from a laser return to the estimated ground

elevation. Canopy height percentiles from 10% to 100% were computed for each quantile and different percentiles density vegetation were similarly calculated.

The data from HRG, HRS, and DMC were examined for geometric distortions prior to image analysis. Then, image data were reprojected into the Swedish National Grid 90 to enable analysis and data extraction at field plot locations. The ALS Digital Terrain Model was used as a complementary source to obtain the CHMs for the two digital surface models (HRS and the photogrammetrically produced height model from DMC images). Thus, CHMs from HRS and DMC data were acquired by subtracting the ground level DEM from above sea level height models

For DMC, the unit conversion was done in ALS data to be the same as DMC canopy height model. In addition, the pixel depth (bit) and image formatting were corrected to perform the digital canopy height subtraction between two digital imageries. For HRS data, resampling was tackled by disaggregating from 20 to 0.5 m pixel size for being able to subtract and compute the pixel-wise raster value. Scale conversion was done for ALS- DEM so that the two images were comparable to perform the subtraction. Besides, pixel depth 16 bit unsigned format equalization was recomputed for two imageries were ensured for canopy height subtraction.

Apart from already processed ALS derived CHM and vegetation ratio, image data from HRG and CHM height data from the CHMs (HRS and DMC) were extracted at each field plot location, using cubic convolution. A few field measured sample plots lying outside the stand boundary, near to the edge of recently clear cut and thinning cut areas were identified as outliers and were removed from further analysis.

2.4. Data Analysis

Multiple linear regressions were applied for all datasets derived from HRG, the CHMs from HRS, DMC, and ALS data. Regression models were developed on the basis of field measured plots and consequently the stand level accuracy assessment was undertaken based on the independent field measured sample plots. Thus, the amount of biomass per hectare was obtained as predicted value. The statistically significant levels were computed related to the mean and coefficient values in terms of backward elimination method till the fewest variables remained in the model. Ordinary least square method was mainly performed for all data analysis at the minimum of 95% confidence interval. Correction of logarithmic bias was applied using the ratio between predicted mean value and actual mean value of the data (Holm, 1977). Furthermore, cross validation was tested to ensure that the functions were not overfitted. Cross validation was computed as a ratio of predicted sum of square of residuals and the ordinary sum of square of residuals (Magnusson, 2005). The mapping accuracy in terms of root mean square error for all model (9 models) formulations was examined.

The result obtained from HRG was used as a benchmark that was again integrated with other sensor data to compare their outcomes. The data fusion applied was between HRG spectral data and canopy height models from HRS, DMC, and ALS data. ALS data was combined with HRG data with and without inclusion of the vegetation ratio as well. The multispectral bands, band ratios, and band squares from HRG were used as independent

variables to predict aboveground biomass. The canopy height models and their logarithm transforms from HRS and DMC were applied as independent variables. For ALS, the various percentile heights (CHM) and vegetation ratio were used as independent variables to model the targeted variable.

A few field plots existing outside the stand polygons due to the DGPS mismatch, field plots that had inconsistent values between spectral values and field measured values, and the inaccurate field plot locations that had big errors were removed to provide reliable estimates. Out of 109 field measured plots for model estimation, 5 and 6 plots were removed for the ALS and DMC data respectively. 96 field measured plots was applied for HRG and up to 97 field measured plots was used in HRS digital surface model to estimate the models. Residual plot studies, cross validation and accuracy assessment were undertaken for all data combinations, including single sensor use and data fusion techniques arising from the combination of two sensors.

3. Results

3.1. SPOT HRG

The four multispectral bands were plotted against the aboveground biomass (b) to acquire an overview of the relationship between spectral bands and the desired predicted variable. The inverse relationship was found as shown in Figure 3, for data extracted at plot level. Hence, the logarithmic transformation of independent variables was applied in order to achieve a linear relation between the modeled variables.

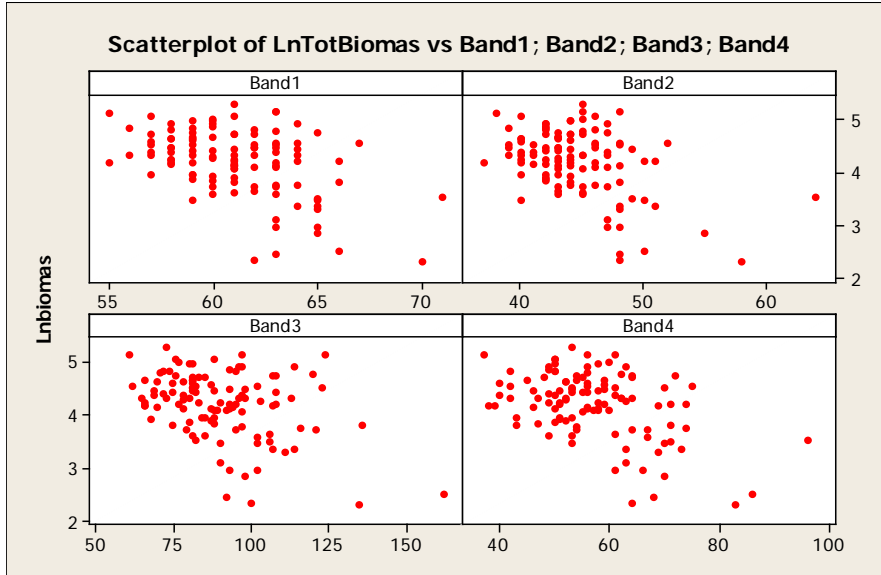


Figure 3. Scatterplots of the HRG bands and biomass (ton/ha).

The correlation values for logarithmically transformed data were higher than untransformed data (Table 4). The correlation values of the band ratios were found higher than the transformed single bands values.

Table 4. Correlation for the four HRG bands to biomass

Variables	$B1$	$B2$	$B3$	$B4$
Biomass(b)	-0.36	-0.32	-0.28	-0.35
$\text{Ln}(b)$	-0.45	-0.44	-0.38	-0.45

In total, 16 variables were applied to develop a model using backward elimination. The model was developed to contain as few variables as possible in conjunction with sufficient significance and highest correlation values. The model is:

$$b = \exp (a_0 + a_1 B1 + a_2 B3 + a_3 B4 + a_4 B4^2 + a_5 B1/B3 + a_6 B3/B4 + \varepsilon) \quad (1)$$

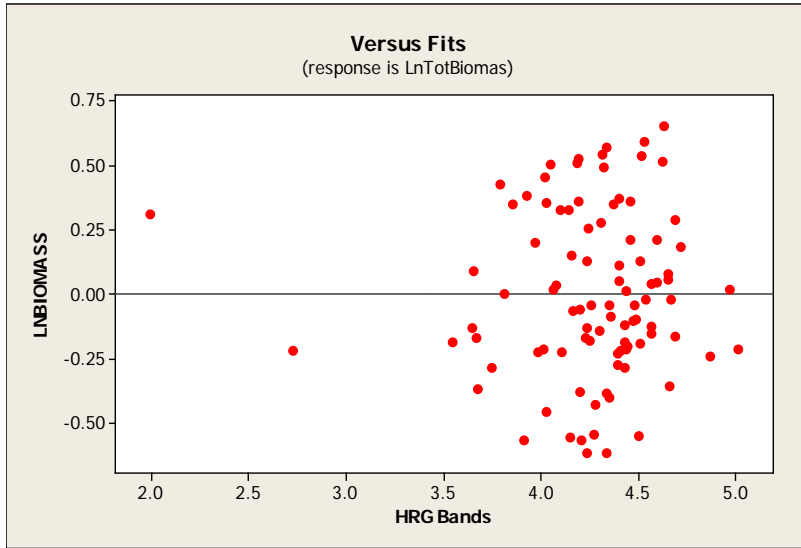


Figure 4. Residual plot of the HRG model

The regression coefficients were all significant ($p \leq 0.001$), and adjusted R^2 was 59.2%.

3.2. SPOT HRS

Five variables were derived from HRS CHM data; the CHM value untransformed (CHM_HRS), the square transformation $(CHM_HRS)^2$, the logarithmic transformation $Ln(CHM_HRS)$, the logarithmic transformation of the square transformation $Ln(CHM_HRS)^2$, and the square transformation of the logarithmic transformation $(Ln_CHM_HRS)^2$, which were plotted to find the highest correlation to biomass. In contrast to other data, such as DMC, HRG, and ALS, the correlation between biomass and CHM_HRS was (0.46) ($p \leq 0.0001$), i.e. higher than for logarithmically transformed data (Table 5).

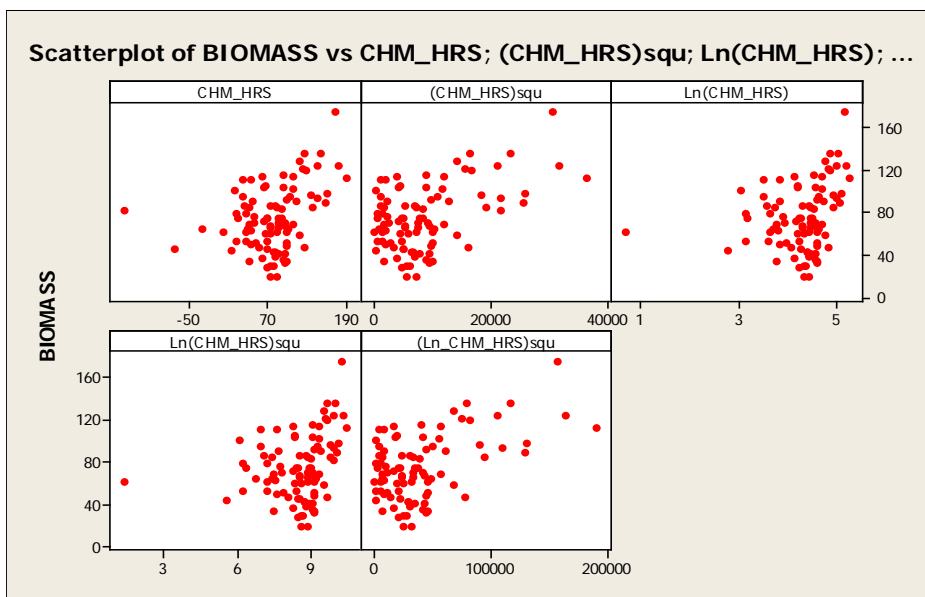


Figure 5. Scatterplots of CHM_HRS and biomass (ton/ha).

Table 5. Correlation for CHM_HRS to biomass

Variables	CHM_HRS	$(CHM_HRS)^2$	$Ln(CHM_HRS)$	$Ln(CHM_HRS)^2$	$(Ln_CHM_HRS)^2$
Biomass(b)	0.31	0.46	0.23	0.22	0.27
$Ln(b)$	0.2	0.34	0.12	0.16	0.12

$(CHM_HRS)^2$ from HRS was regressed to the biomass, b and resulted in an R^2 of 23% and was significant ($p < 0.0001$).

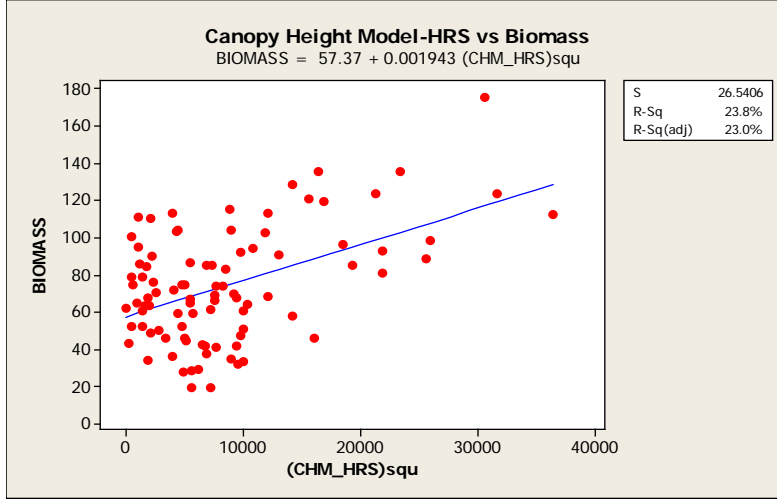


Figure 6. Scatterplot of estimated biomass from CHM_HRS data and true biomass (ton/ha)

The model obtained from HRS is expressed as

$$b = \alpha_0 + \alpha_1 CHM_HRS^2 + \varepsilon \quad (2)$$

3.3. Z/I DMC

Five variables derived from DMC data were used as CHM value untransformed (CHM_DMC), the square transformation (CHM_DMC^2), the logarithmic transformation $Ln(CHM_DMC)$, the logarithmic transformation of the square transformation $Ln(CHM_DMC)^2$, and the square transformation of the logarithmic transformation ($Ln_CHM_DMC^2$). The $(Ln_CHM_DMC)^2$ showed the highest correlation; 0.87 ($p \leq 0.0001$) to logarithmically transformed biomass (Table 6), and was chosen for model (Eq. 3). The regression coefficients were significant ($p \leq 0.0001$) and the adjusted R^2 was 77.7%.

$$b = \exp(\alpha_0 + \alpha_1(Ln_CHM_DMC)^2 + \varepsilon) \quad (3)$$

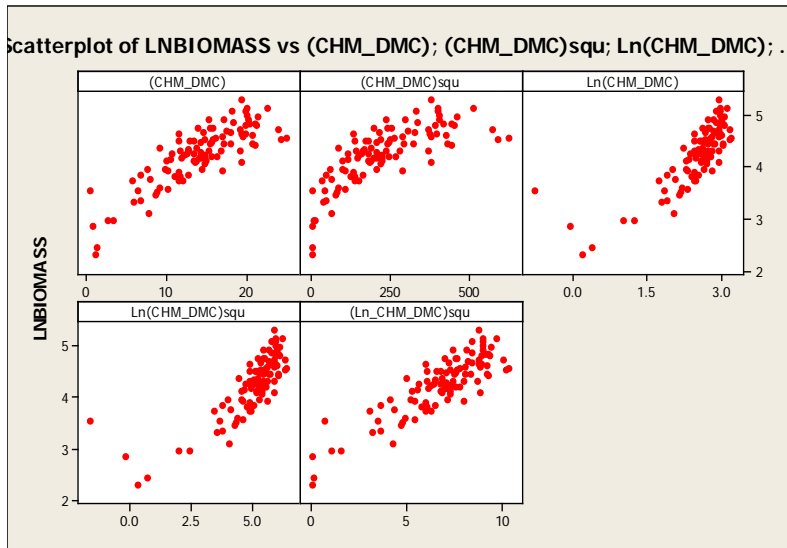


Figure 7. Scatterplots of CHM_DMC and biomass (ton/ha).

Table 6. Correlation for CHM_DMC to biomass

Variables	<i>CHM_DMC</i>	$(CHM_DMC)^2$	$Ln(CHM_DMC)$	$Ln(CHM_DMC)^2$	$(Ln_CHM_DMC)^2$
Biomass(<i>b</i>)	0.78	0.75	0.67	0.65	0.76
$Ln(b)$	0.84	0.76	0.8	0.8	0.87

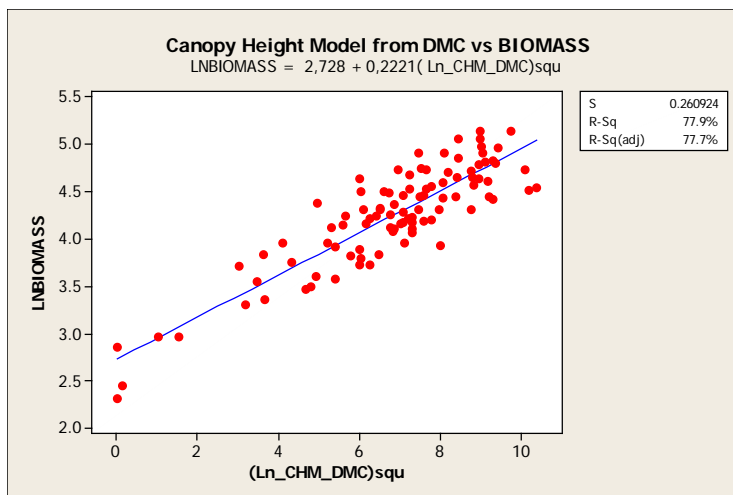


Figure 8. Scatterplot of estimated biomass from CHM_DMC data and true biomass (ton/ha).

3.4. ALS (Canopy Height Model)

The 22 variables of percentile height (*CHM_10*, *CHM_20*,, *CHM_100*) were plotted against the biomass data and all showed positive correlation.

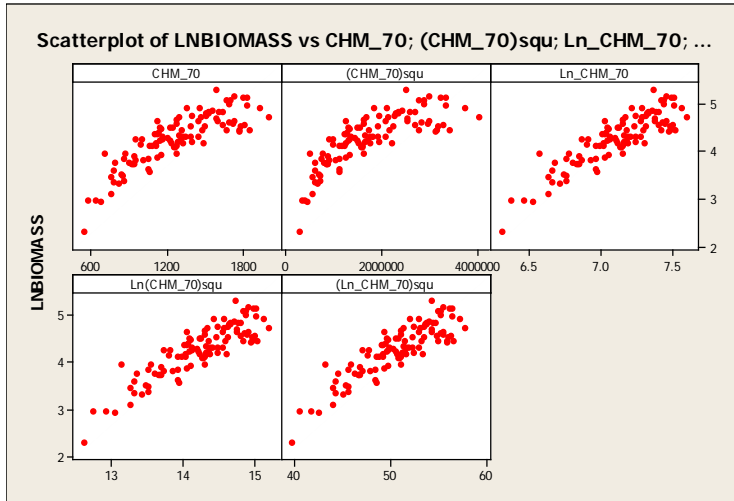


Figure 9. Scatterplots of CHM_ALS and biomass (ton/ha).

Logarithmic transformation of CHM (Ln_CHM) was higher correlation than logarithmic untransformed biomass. Of these, logarithmic transformation of 70 percentile CHM (Ln_CHM_70) showed the highest correlation to biomass (Table 7).

Table 7. Correlation for CHM_ALS to biomass

Variables	CHM_70	$(CHM_70)^2$	Ln_CHM_70	$Ln(CHM_70)^2$	$(Ln_CHM_70)^2$
Biomass (b)	0.77	0.75	0.77	0.75	0.76
$Ln(b)$	0.79	0.71	0.84	0.71	0.83

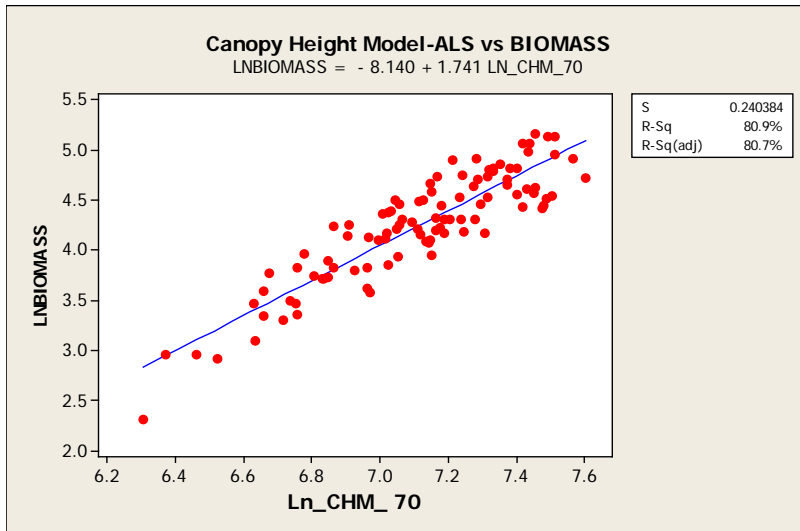


Figure 10. Scatterplots of estimated biomass from CHM_ALS data and true biomass (ton/ha).

The regression coefficients were significant ($p \leq 0.0001$) and resulted in 80.7% of R^2 (Eq. 4).

$$b = \exp(\alpha_0 + \alpha_1 Ln_CHM_70 + \varepsilon) \quad (4)$$

3.5. SPOT HRS and SPOT HRG

The canopy height models from HRS and 16 variables from HRG were plotted against biomass to assess the correlation.

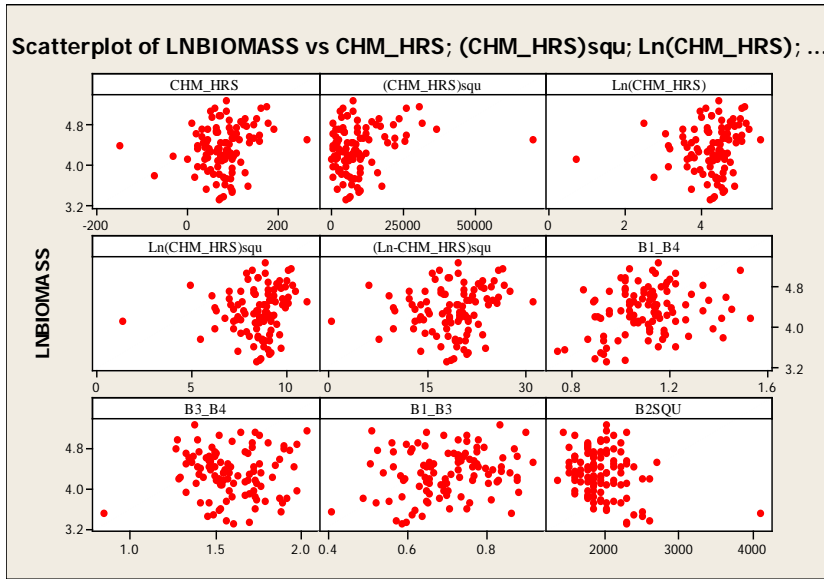


Figure 11. Scatterplots of CHM_HRS and HRG data to biomass (ton/ha).

$(CHM_HRS)^2$, 3 pairs of band ratios and band 2 were selected to fit the model with logarithmically transformed biomass (Table 8).

The total of 21 variables from combined *CHM_HRS* and HRG data were regressed to biomass (*b*) showing significance (95% confidence interval) (Eq. 5).

Table 8. Correlation CHM_HRS and HRG to biomass

Variable	$(CHM_HRS)^2$	$Ln(CHM_HRS)$	$B1/B3$	$B1/B4$	$B3/B4$	$B2^2$
Biomass (<i>b</i>)	0.46	0.23	0.23	0.22	0.28	-0.36
$Ln(b)$	0.34	0.12	0.34	-0.35	0.37	-0.45

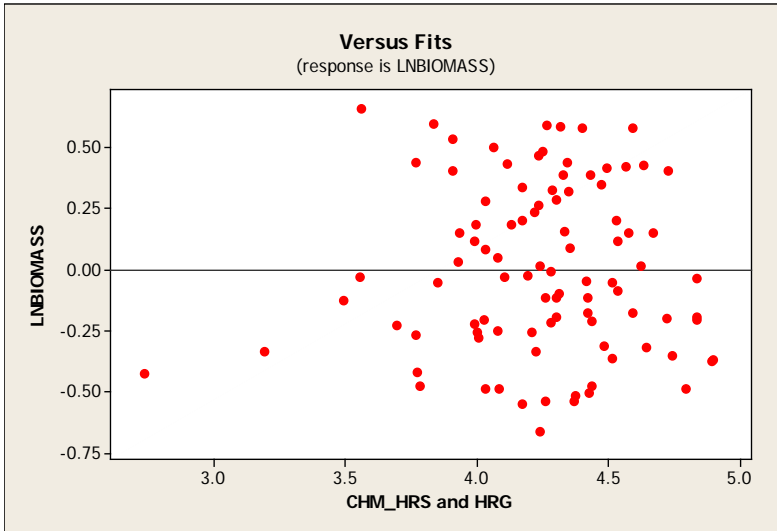


Figure 12. Residual plot of the CHM_HRS and HRG model.

$$b = \exp (\alpha_0 + \alpha_1 (CHM_HRS)^2 + \alpha_2 B1/B4 + \alpha_3 B3/B4 + \alpha_4 B2^2 + \alpha_5 B1/B3 + \varepsilon) \quad (5)$$

Apart from the constant value, all coefficient regression values were significant ($p \leq 0.001$). Adj R^2 increased to 50.2% from 23% and RMSE improved from 35.4% to 26.9%.

3.6. Z/I DMC and SPOT HRG

The canopy height model from DMC (CHM_DMC) and 16 variables from HRG were plotted against the aboveground biomass. The logarithmically transformed values for height were higher relative to logarithmic transformed biomass (Table 9).

The model was developed from 18 independent variables from HRG data and CHM from DMC to model biomass, using the same regression modeling approach method as described previously.

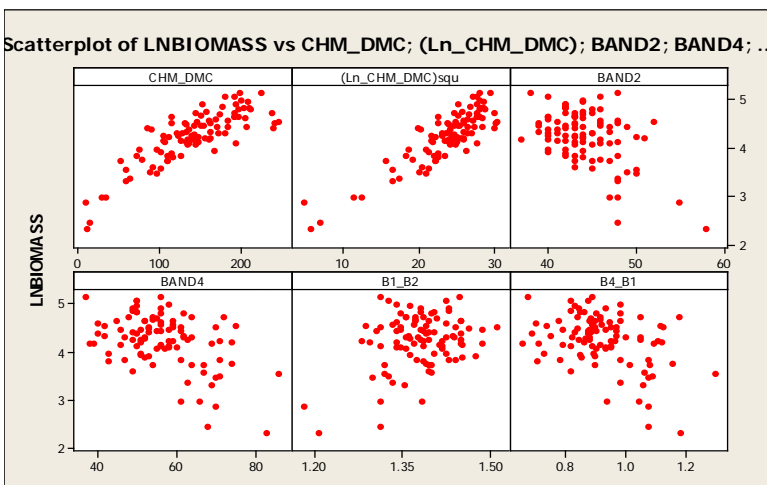


Figure 13. Scatterplots CHM_DMC and HRG data to biomass (ton/ha).

Table 9. Correlation of CHM_DMC and HRG Data to biomass

Variables	$(Ln_CHM_DMC)^2$	$B2$	$B4$	$B1/B2$	$B4/B1$
Biomass (b)	0.76	-0.32	-0.35	0.19	-0.33
$Ln(b)$	0.87	-0.45	-0.45	0.33	-0.39

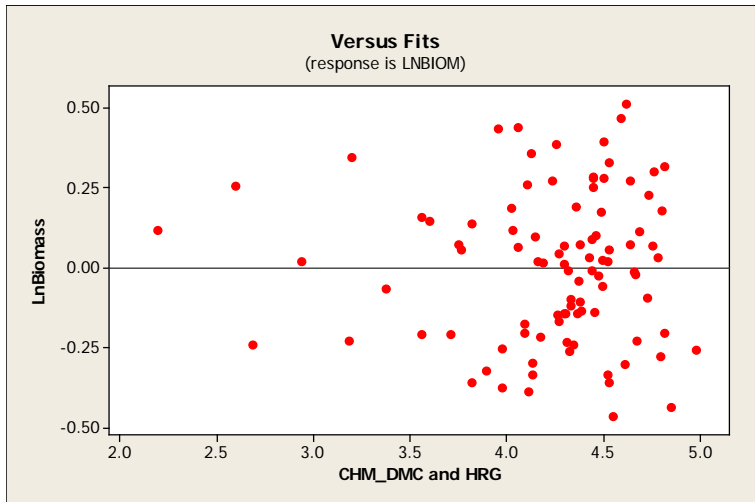


Figure 14. Residual plot of the CHM_DMC and HRG model.

The resulting model is

$$b = \exp (\alpha_0 + \alpha_1(Ln_CHM_DMC)^2 + \alpha_2 B2 + \alpha_3 B4 + \alpha_4 B1/B2 + \alpha_5 B4/B1 + \varepsilon) \quad (6)$$

All regression coefficients were significant ($p \leq 0.05$) and the coefficient of determination was 80.0%.

3.7. ALS (Canopy Height Model) and SPOT HRG

Combination of sixteen variables from HRG and 22 variables from ALS height data (CHM) were plotted against biomass. Logarithmically transformed values for single bands were also introduced. However, the result is more or less the same with or without including the logarithmic transformation of spectral bands.

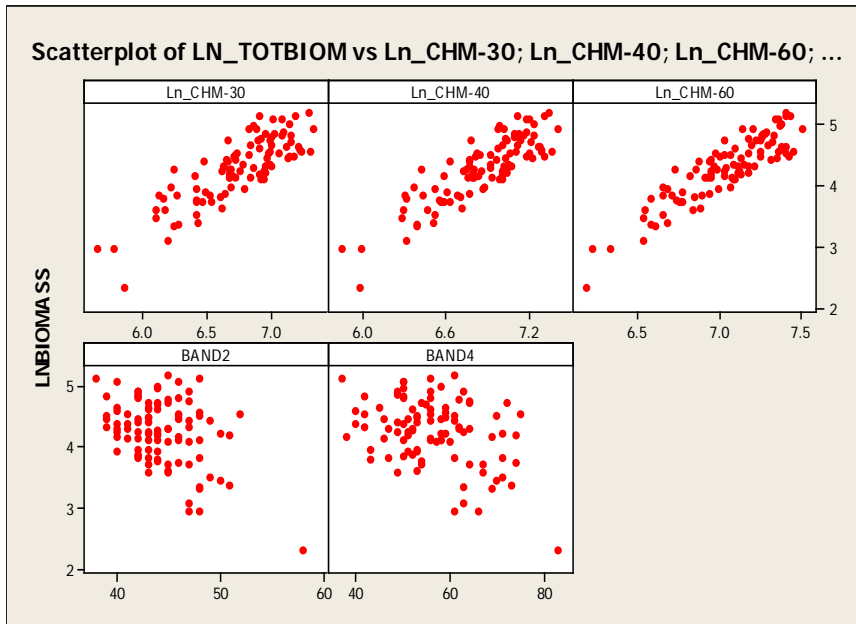


Figure 15. Scatterplots of CHM_ALS and HRG to biomass (ton/ha).

The variables selected for the fused regression model was *B2* and *B4* in combination with the *CHM_30*, *CHM_40*, and *CHM_60* percentile heights (Table 10).

Table 10. Correlation of ALS_CHM and HRG Data to biomass

Variables	<i>Ln_CHM_30</i>	<i>Ln_CHM_40</i>	<i>Ln_CHM_60</i>	<i>Band2</i>	<i>Band4</i>
Biomass (<i>b</i>)	0.71	0.73	0.77	-0.32	-0.35
Ln(<i>b</i>)	0.78	0.80	0.83	-0.44	-0.45

The model was developed using the previously described method, and resulted in significance ($p \leq 0.001$) for regression coefficients, except *Band4*, which was significant ($p \leq 0.05\%$) (Eq. 7). The coefficient of determination was 84.5%.

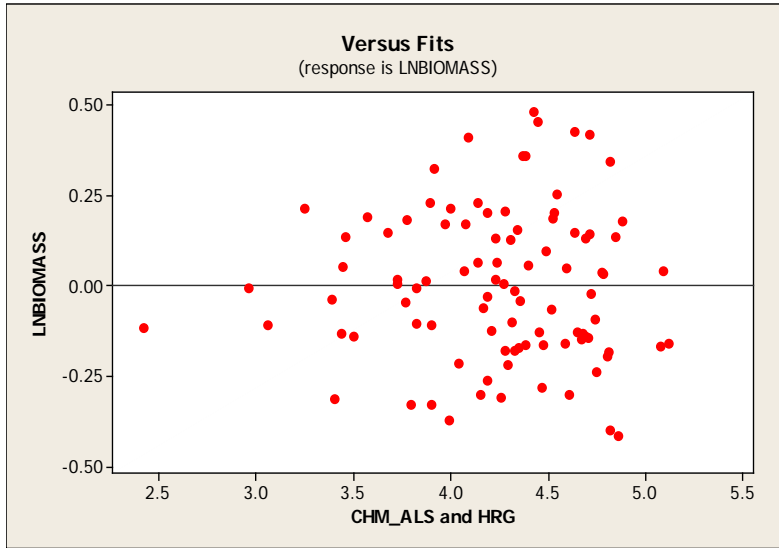


Figure 16. Residual plot of the CHM_ALS and HRG model.

The model obtained from CHM_ALS and HRG is described as Equ.7.

$$b = \exp (\alpha_0 + \alpha_1 \text{Ln_CHM_30} + \alpha_2 \text{Ln_CHM_40} + \alpha_3 \text{Ln_CHM_60} + \alpha_4 B2 + \alpha_5 B4 + \varepsilon) \quad (7)$$

RMSE improved from 20.2% to 15.6% when the combined biomass estimates was undertaken.

3.8. ALS (Canopy Height Model and Vegetation Ratio)

Here, the ALS CHM variables were used and complemented with the vegetation ratio variable, in order to assess the accuracy from using all available ALS data. Adding vegetation ratio to the model improved the coefficient of determination from 80% to 90.5%, and the stand-level prediction accuracy from 20% to 15.7% RMSE. The regression coefficients were all significant at ($p \leq 0.001\%$).

Table 11. Correlation of ALS_CHM_Veg to Biomass

Variables	<i>Ln_CHM_30</i>	<i>Ln_CHM_90</i>	<i>Ln_Veg</i>
Biomass (b)	0.71	0.77	0.70
Ln(b)	0.78	0.83	0.78

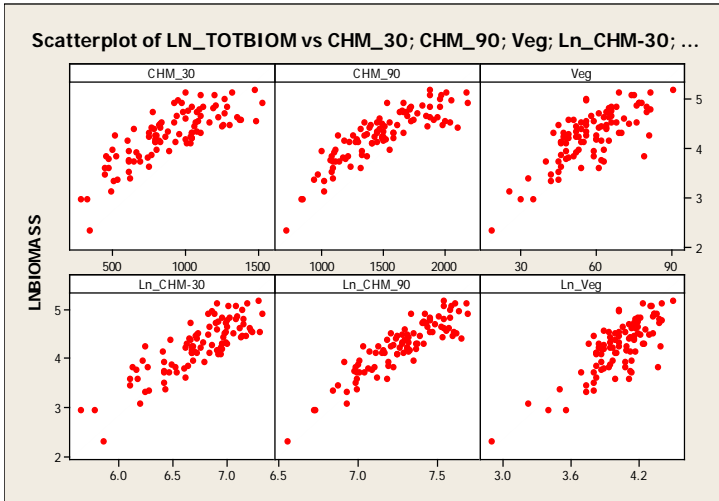


Figure 17. Scatterplots of ALS (CHM & Veg) to biomass (ton).

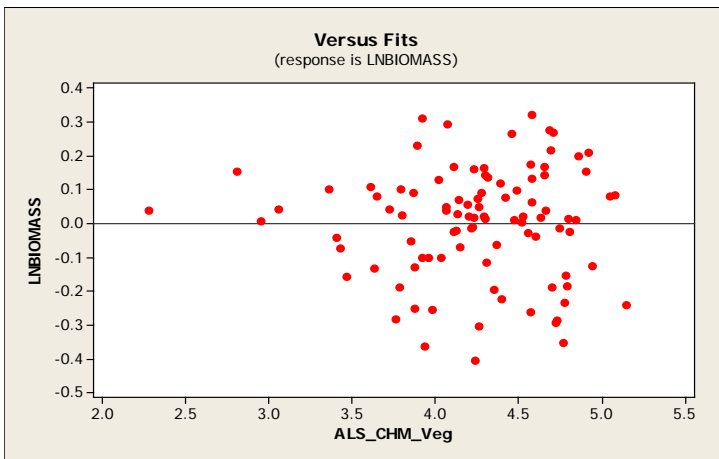


Figure 18. Residual plot of the model using ALS CHM and vegetation ratio.

To fit the model, the selected variables are logarithmically transformed 30 percentile height data (Ln_CHM_30), (Ln_CHM_90), and logarithmically transformed vegetation (Ln_Veg).

The resulting model for ALS CHM and vegetation ratio is;

$$b = \exp (\alpha_0 + \alpha_1 Ln_CHM_30 + \alpha_2 Ln_CHM_90 + \alpha_3 Ln_Veg + \varepsilon) \quad (8)$$

3.9. ALS (Canopy Height Model and Vegetation Ratio) and SPOT HRG

Thirty nine variables including vegetation ratio were used for model development. Selected variable correlations with and without transformation of biomass are showed in Table 12. The highest correlation of the logarithmically transformed 70 percentile height data (Ln_CHM_70) and the logarithmically transformed biomass was 0.84.

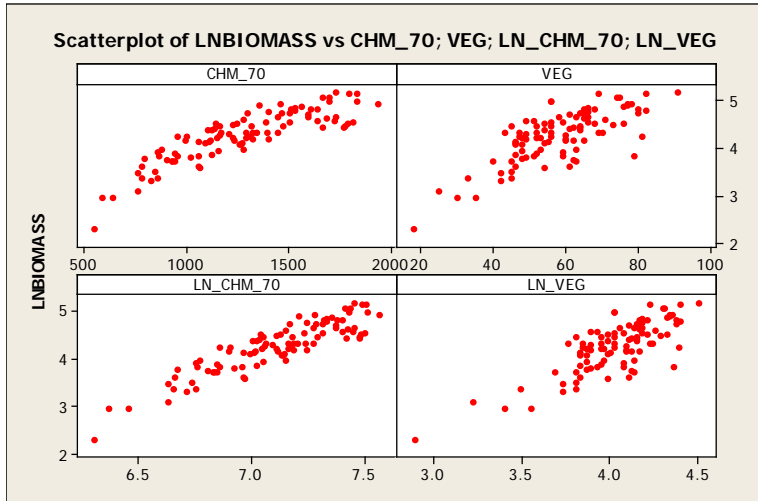


Figure 19. Scatterplot of ALS_CHM_Veg and HRG data to biomass (ton/ha).

Table12. Correlation of ALS_CHM_Veg and HRG data to biomass

Variables	Ln_CHM_70	Ln_Veg	$B4$
Biomass (b)	0.77	0.70	-0.35
$Ln(b)$	0.84	0.78	-0.45

The best predictors found are logarithmically transformed *percentile height 70* (Ln_CHM_70), band 4 ($B4$) and *logarithmic vegetation ratio* (Ln_Veg) (Eq. 9). They were significant at ($p \leq 0.001$) except $B4$ which was significant ($p \leq 0.01$) in regression model.

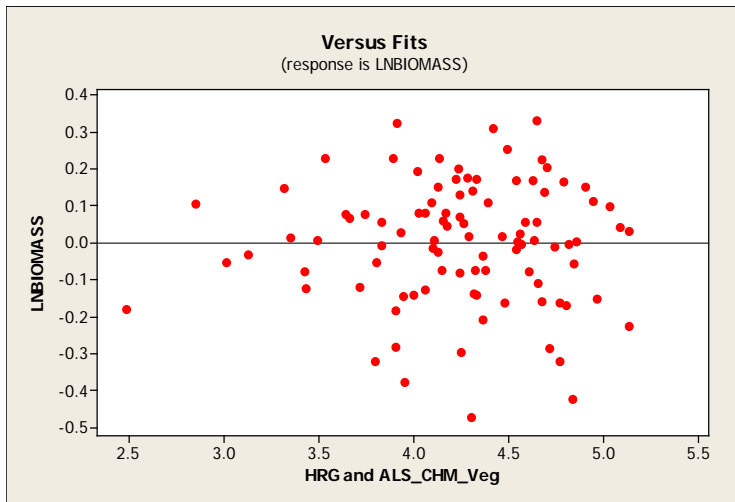


Figure 20. Residual plot of ALS_CHM_Veg and HRG model.

The combined biomass estimate of regression model is expressed as follow,

$$b = \exp (\alpha_0 + \alpha_1 B4 + \alpha_2 Ln_CHM_70 + \alpha_3 Ln_Veg + \varepsilon) \quad (9)$$

When the vegetation ratio is included in the model, RMSE decreased compared to model 8 (15.7% to 14.1%), and the coefficient of determination increased from 84.5% to 90.2%.

Stand level prediction performance of the 9 regression models is presented in Table 13, in terms of RMSE, adjusted coefficients of determination and cross validation value q . Apart from the intercept, α_0 , of model 5, all regression parameters were significant at the 0.001% or 0.05% significance level. Cross validation undertaken for all models were found within the standard limit ($q \leq 1.04$ and $q \leq 1.15$) that imply the models were not overfitted. The correspondent regression coefficients are presented in order of models 1 to 9 in Table 15.

Table13. Regression coefficients (α_0 - α_6), and significance level for logarithmic aboveground biomass regression functions derived from models (1)-(9) based on 109 field plots

Model	α_0	α_1	α_2	α_3	α_4	α_5	α_6
1	-34.58***	-0.32***	-57***	0.822***	-0.004***	19.4***	11***
2	57.37***	0.001***					
3	1.823***	0.101***					
4	-8.14***	1.741***					
5	-1.01(ns)	0.0001***	-7.95***	4.55***	-0.001***	12.5***	
6	-18.8***	0.09***	0.254***	-0.254*	7.11***	15.3**	
7	-3.01***	3.5***	-5.68***	3.55***	-0.06***	0.007*	
8	-9.26***	0.296***	1.15***	0.77***			
9	-5.82***	-0.005**	1.34***	0.0135***			

Notes; Significant levels: $p \leq 0.05\%$ (*), $p \leq 0.01\%$ (**), $p \leq 0.001\%$ (***) , ns = not significant

Stand-level prediction performance, in terms of RMSE and coefficients of determination, for each model are presented in Table 14. Using HRG data only, the RMSE accuracy and R^2 (i.e. of the relation between predicted and true stand biomass) obtained were 31.8% (27.9 ton/ha) and 60% respectively, using model 1 which contained spectral bands B1, B3, B4, the square of B4 and the band ratios B1/B3 and B3/B4. The logarithmically transformed values of B1, B2, and B4 showed approximately similar correlation coefficients ($r = 0.45$).

Comparing models utilizing CHM data only, the model of DMC CHM showed the lowest prediction errors: 18.79% (15.8 ton/ha) RMSE, followed by ALS showing 20.25% (17.77 ton/ha), and 35.4% (31.1 ton/ha) for HRG CHM (model 3, 4, and 2). Corresponding coefficients of determinations were 77%, 80.7% and 23% for Z/I DMC, ALS and HRS.

Table14. RMSE, (Adj R^2), and q values for logarithm Abg biomass functions of 1-9 models

Models	Sensor	RMSE(%)	Adj. R ²	<i>q</i>
1	SPOT HRG	31.9	60.0	1.15
2	SPOT HRS	35.4	23.0	
3	Z/I-DMC (<i>CHM</i>)	18.8	77.0	1.04
4	ALS (<i>CHM</i>)	20.2	80.7	1.04
5	SPOT HRS + SPOT HRG	26.9	50.2	1.15
6	Z/IDMC (<i>CHM</i>) + SPOT HRG	16.9	80.0	1.15
7	ALS (<i>CHM</i>) + SPOT HRG	15.6	84.5	1.15
8	ALS (<i>CHM</i> + <i>Vegetation ratio</i>)	15.7	90.5	1.04
9	ALS (<i>CHM</i> + <i>Vegetation ratio</i>) + SPOT HRG	14.1	90.2	1.15

For the data fusion models, HRG and CHM data from HRS, DMC and ALS were evaluated. At first various percentiles heights from ALS were used without including the *vegetation ratio* variable. Accuracy was then improved from 35.4% to 26.9% using HRS, from 18.7% to 16.9% using DMC and from 20.25% to 15.7% using ALS, when each of these variables were combined with HRG corresponding to the model 5, 6 and 7. The corresponding stand-level prediction RMSE were 23.6 ton/ha for model 5, 14.8 ton/ha for model 6, and 13.7 ton/ha for model 7. At the same time, the values of R² were increased from 20.1% to 50%, from 77% to 80%, and from 80.4% to 84.5%, for HRS, DMC, and ALS data, respectively. The predictor *vegetation ratio* was not utilized for ALS data in model 7.

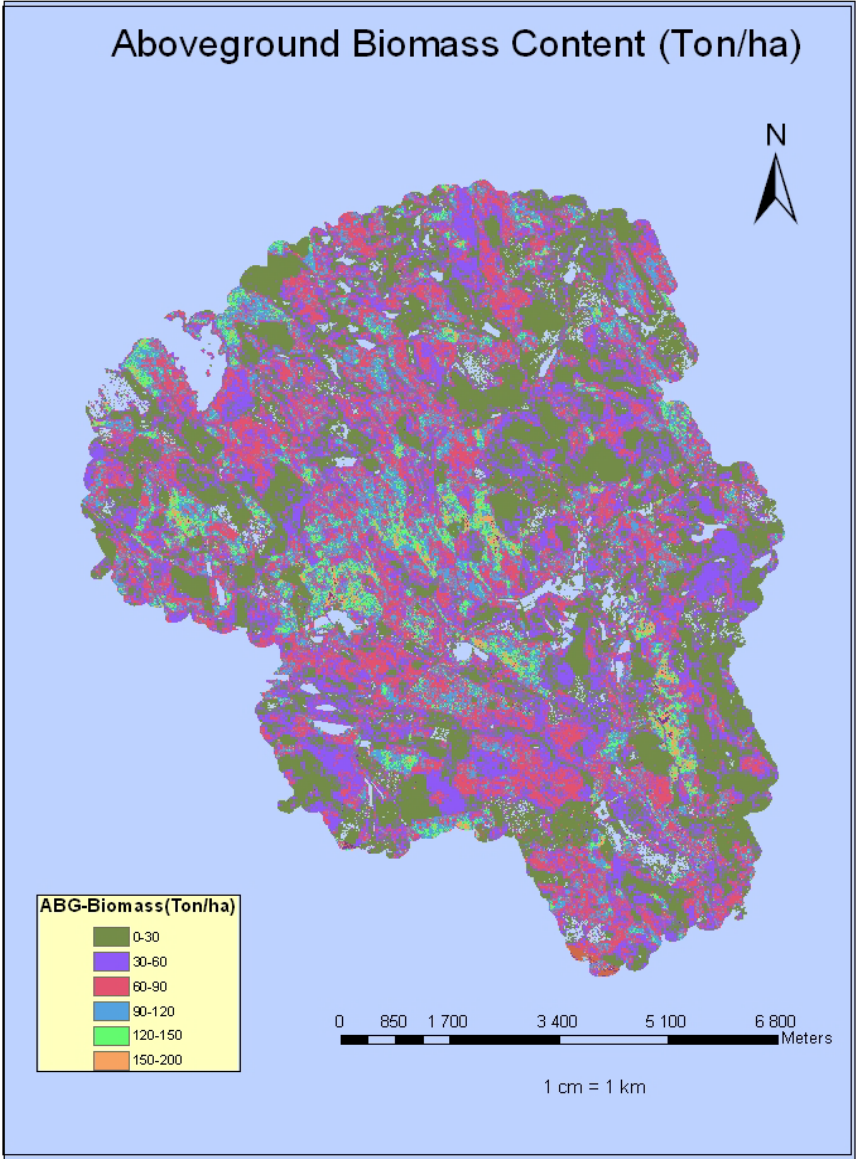
Models 8 and 9 were computed for ALS data including various percentile heights in combination with *vegetation ratio*. Performance of both ALS data only, and in combination with HRG data were evaluated. Stand-level prediction accuracy of 15.7% RMSE and 90.5% R² were found using ALS including vegetation ratio. Adding HRG data to this model improved the accuracy from 15.7% to 14.1% RMSE (model 9). The coefficient of determination was similar to model 8. The prediction error obtained using ALS data only was 13.8 ton/ha and 12.4 ton/ha for the combination of both sources.

Table15. Regression models

No Models

- (1) $b = \exp (34.5 + 0.324 B1 + 0.0569 B3 + 0.822 B4 + 0.00428 B4^2 + 19.4 B1/B3 + 11.0 B3/B4 + \varepsilon)$
- (2) $b = 57.37 + 0.001 (CHM_HRS)^2 + \varepsilon$
- (3) $b = \exp (2.72 + 0.22 (Ln_CHM_DMC)^2 + \varepsilon)$
- (4) $b = \exp (8.14 + 1.741 Ln_CHM70 + \varepsilon)$
- (5) $b = \exp (1.01 + 0.00011 CHM_HRS^2 + 7.95 B1/B4 + 4.55 B3/B4 + 0.0010 (B2)^2 + 12.5 B1/B3 + \varepsilon)$
- (6) $b = \exp (18.8 + 0.0917 (Ln_CHM_DMC)^2 + 0.254 B2 + 0.254 B4 + 7.11 B1/B2 + 15.3 B4/B1 + \varepsilon)$
- (7) $b = \exp (3.01 + 3.50 Ln_CHM_30 - 5.68 Ln_CHM_40 + 3.55 Ln_CHM_60 + 0.06 B2 + 0.008 B4 + \varepsilon)$
- (8) $b = \exp (9.26 + 0.296 Ln_CHM_30 + 1.15 Ln_CHM_90 + 0.77 Ln_Veg + \varepsilon)$
- (9) $b = \exp (5.82 + 0.00502 B4 + 1.34 Ln_CHM_70 + 0.0135 Ln_Veg + \varepsilon)$

The models resulting from the different combinations of remotely sensed data are shown in Table 15. Using the best performing model, of ALS and HRG data, a map of biomass was made for the area (Figure 21).



Map of Aboveground Biomass Distribution in Krycklan, Sweden

Figure 21. Map of Aboveground Forest Biomass Distribution in Krycklan Area.

4. Discussion and Conclusions

Providing timely and accurate data in order to formulate forest management plans and monitor forest resources for the sake of economical return, ecological stability and social values is of high importance for solving many issues related to sustainable use of natural resources. Planning and monitoring the existing resources and changes with time can cost-efficiently be made of large areas, and be applied in regional, national and global scales. For this purpose, spaceborne and airborne remote sensing are being combined with NFI and other field measured data to map different forest variables. Airborne ALS is one of the most promising sources, which may be combined with data from other sensors to produce more precise and accurate information needed for a broad range of purposes. Previously untested digital surface model data from Z/I DMC and SPOT HRS provided new results in this study, when applied for estimation of dry woody biomass in combination with multispectral data from SPOT HRG.

The use of SPOT HRG included single bands, band ratios, and band squares. The result from SPOT HRG was consistent with previous studies in stem volume estimation in Swedish boreal and temperate forest using SPOT, Landsat TM and/or ETM+ in the *k*NN non-parametric estimation method typically produced 24-32% RMSE stand-level accuracy (Magnusson, 2006; Reese et. al 2002). Using the optical satellite sensors SPOT HRVIR, SPOT HRG, and Landsat ETM+ showed similar outcomes for mapping stem volume in Swedish forests, ranging from 23 to 32% RMSE (Fransson et. al 2004). The application of Landsat TM data in combination with NFI field plot measurements data predicting forest volume and biomass at Kättböle in Sweden resulted about 66% RMSE (Fazakas et al 1999) at plot level. However, the aggregation of RMSE assessment for the complete 510 ha large area was 8.7% for biomass. Muukkonen and Heiskanen (2005) reported 41-44.4% RMSE using ASTER image data (9 bands) with the emphasis on non-linear multiple regression and natural networks in Southern boreal forest in Finland. The spatial resolutions used in this research were 15, 30 and 90 m for the visible near infrared, shortwave infrared and thermal infrared bands, respectively. Aboveground biomass estimated using visible to shortwave infrared advanced spaceborne thermal emission and reflection radiometer (ASTER) data in Finland was reported to be made with 41% RMSE as the best (Heiskanen, 2006).

SPOT HRS alone predicted with 35.4% (31.1 ton/ha) RMSE accuracy. Combining SPOT HRS CHM and HRG data improved the accuracy by 24% corresponding to 21.1 ton/ha. Using the combination of HRS CHM and HRG was more or less equivalent to the use of other medium spatial resolution optical sensors (Landsat TM/ETM+, SPOT). Since its use is simpler and easier due to one variable regression analysis, CHM data from HRS has a new potential to be used in the future.

Z/I DMC CHM data rendered the lowest prediction error among three canopy height models of HRS, DMC, and ALS. Accuracy obtained from DMC was 18.79% (15.8 ton/ha) RMSE. This result of accuracy assessment was comparable to the use of medium to fine resolution sensor use in estimating aboveground biomass. The use of ALS data for biomass estimation in boreal forest in Norway was found to be 21% RMSE (Næsset, 2008). Magnusson and Fransson (2004) found that predicted error (RMSE) of stem volume at the stand level assessment was 18-24% using of aerial photo interpretation and 16% by using a

combination of CARABAS and SPOT HRVIR, results comparable to the data integration of canopy height DMC and SPOT HRG results of 16.9% RMSE from this study.

The use of ALS derived canopy height model without *vegetation ratio* resulted in 80.7% R^2 and a prediction error of 17.77 ton/ha corresponding to the 20.25% of RMSE. However, R^2 improved from 80.7% to 90.5% and the prediction error improved from 20.25% to 15.7% when *vegetation ratio* was included in the aboveground biomass regression model. This result is consistent with and even a bit better than aboveground biomass prediction in southern Norway by Næsset (2008) in which R^2 was 88% and RMSE 21% based on the ALS derived variables.

The accuracy was even higher - 15.7% to 14.1% (12.4 ton/ha) in our study when ALS data was combined with SPOT HRG spectral bands. The variance of biomass was explained by 90.2% (adj. R^2) by the prediction. This result is comparable and consistent with 90% R^2 and 22% of RMSE of stem volume estimation in southern part of Sweden by Holmgren (2003) where ALS derived mean height and crown coverage were used as predictors at plot level.

The result from the combination of SPOT HRG and ALS data was consistent with the previous study by Wallerman and Holmgren (2007) who reported 20% RMSE for stem volume estimation in southern part of the Sweden using ALS and SPOT HRG data. The accuracy of 10% was increased when the *vegetation ratio* was included in ALS data combined with SPOT HRG in the present study. The difference between the current study and the work done by Wallerman and Holmgren (2007) and Holmgren (2003) was that their study area is located in the southern part of Sweden and stem volume predict and that they estimated stem volume rather than biomass.

The results acquired from the digital surface models were reliable and could be applicable for future use since the accuracy from DMC canopy height predictor was comparable to the use of canopy height data alone from ALS. The situations of study sites between previous studies and this are slightly different even though the prevailing tree species and biophysical conditions are the similar. However, the boreal forests in northern America are different and the remote sensing data could be applicable and comparable regardless of the some differences in forest condition like species composition, number of species (species diversity), given that stem volume per hectare is more or less the same.

The highest accuracy and R^2 was found in ALS data with the inclusion of *vegetation ratio* as predictor in conjunction with different percentile canopy heights. Combined with SPOT HRG, the error was reduced to 14.1% and over 90% of the variability in biomass was explained by the predictions.

The combined predictors of ALS height percentiles and *vegetation ratio* produced the best accuracy (RMSE) and highest coefficient of determinations compared to the use of ALS height percentiles alone. Furthermore, ALS data produced the highest accuracy among all sensors in our study with the inclusion of *vegetation ratio*.

ALS data predicted aboveground biomass accurately in combination with SPOT HRG data since the ALS provide both horizontal and vertical dimensions which are of importance for the function of biomass estimation from crown, branches, and foliages and stem and so on. The accuracy improvement by combining ALS and SPOT HRG was a little more than the use of ALS data alone - from 15.7% to 14.1% RMSE. Prediction error from the combination of DMC CHM and HRG was comparable to the ALS height data and HRG integration providing 16.9% and 15.6% respectively. The main task of this study was to assess aboveground biomass accuracy at stand level using various remotely sensed data acquired from the digital surface canopy heights (SPOT HRS and Z/I DMC), multispectral bands from SPOT HRG imagery and small foot print ALS data. Both individual sensor data and combinations of sensors were applied to assess the aboveground biomass estimation accuracy. Single datasets used in this study were HRG, HRS canopy height model, Z/I-DMC CHM, and ALS CHM with and without inclusion of *vegetation ratio*. The applied combinations/models were (i) SPOT HRG and CHM from SPOT HRS, (ii) SPOT HRG and DMC CHM, (iii) SPOT HRG and ALS CHM (iv) SPOT HRG and ALS CHM and *vegetation ratio*. The various percentile heights (CHM) and *vegetation ratio* from ALS were administered separately so that the results with and without *vegetation ratio* can be compared with other digital surface model outputs obtained from SPOT HRS and DMC. The central part of this study was to evaluate the enhancement of biomass prediction relative to multispectral bands reflectance of SPOT HRG combined with the digital surface models from SPOT HRS and Z/I DMC data.

Combining sensors is found effective and efficient in terms of accuracy and cost for estimation for all datasets. The emphasis in the current study was placed on the use of digital surface models from SPOT HRS and Z/I DMC which were found potential for future use. The mapping accuracy improved reliably when the digital surface model from each sensor was combined with multispectral bands application from SPOT HRG to predict dry weight of woody forest biomass.

RMSE and R^2 were improved when CHM data were used in combination with HRG data, both for SPOT HRS and DMC CHM. The results derived from height models were reliable and comparable to other medium and fine pixel size sensors use. For some cases, the output was better showing about 16% accuracy improvement compared to estimation from optical sensor data, including digital aerial photographs, in other research papers. Thus, integration of digital surface models and multispectral bands from satellite and airborne sensors may provide a new way to estimate aboveground biomass and consequently to monitor carbon sinks and sequestration in boreal forest. In addition, the use of optical sensors is cost effective and may readily be applied to monitor the biophysical properties in the local, regional and national scales.

Future research may provide further improvements, such as investigation of DMC and ALS derived variables such as crown diameter, number of stems and various percentile heights. In addition, the vegetation indices like textural values from both SPOT HRG and DMC could be combined with ALS derived data to predict the various biophysical variables including woody biomass to gain improved insight about the functions of these variables for future outlook. Woody biomass prediction may be done in different forest types and different age classes relative to species specific variation in Sweden in order to distinguish, for instance, carbon sink potentials for each species with respect to age class and forest type.

Acknowledgements

I am grateful to my supervisor Dr. Jörgen Wallerman for his constructive feedbacks and continuous guidance throughout the entire research work. I like to thank Professor Håkan Olsson who provided this research framework and valuable suggestions for this work. I like to thank Associate Professor Sören Holm for fruitful discussion on statistical analysis. My thanks also extend to the GIS coordinator Mats Högström for his support in data management and preparation in the use of Arc GIS software. I wish to thank the teachers and researchers from Forest remote sensing section for their kind responses and discussions whenever a question was raised. SPOT5 HRS Digital Surface Model was provided by Centre National d'Études Spatiales (CNES) Agency, France. Two year Master of Science in European Forestry Program including thesis work was financially supported by European Commission.

References

- Åge, P.J. 1985. Forest Inventory Photo Interpretation. National Land Survey, Sweden, LMV Report 13. 21pp.
- Bouillon, A., Bernard, M., Gigord, P., Orson, A., Rudowski, V., & Baudoin, A. 2006. SPOT 5 HRS geometric performances: Using block adjustment as a key issue to improve quality of DEM generation. *ISPRS Journal of Photogrammetry & Remote Sensing* 60, 134-136.
- Chen, D.M. & Stow, D. 2003. Strategies for integrating information from multiple spatial resolutions into land-use/land-cover classification routines. *Photogrammetric Engineering and Remote Sensing* 69, 1279-1287.
- Fazakas, Z., Nilsson, M. & Olsson, H. 1999. Regional forest biomass and wood volume estimation using satellite data and ancillary data. *Agricultural and Forest Meteorology* 98-99, 417-425.
- Foody, G.M. 2003. Remote sensing of tropical forest environments: towards the monitoring of environmental resources for sustainable development. *International Journal of Remote Sensing* 20, 4035 – 4046.
- Garcia, M., Riaño, D., Chuvieco, E., & Danson, F.M. 2010. Estimating biomass carbon stocks for a Mediterranean forest in central Spain using LiDAR height and intensity data. *Remote Sensing of Environment* 114, 816-830.
- Gong, P. 1994. Integrated analysis of spatial data from multiple sources: an overview. *Canadian Journal of Remote Sensing* 20, 349-359.
- Hall, R.J., Skakun, R.S., Arsenault, E.J. & Case, B.S. 2006. Modeling forest stand structure attributes using Landsat ETM+ data: Application to mapping of aboveground biomass and stand volume. *Forest Ecology and Management* 225, 378-390.
- Heiskanen, J. 2006. Estimating aboveground tree biomass and leaf area index in a mountain birch forest using ASTER satellite data. *International Journal of Remote Sensing* 6, 1135-1158.
- Holm, S. 1977. Transformationer av en eller flera beroende variabler i regressionsanalys, HUGIN Rapport nr 7, Swedish University of Agricultural Sciences, Stockholm, Sweden, 21 pp. (in Swedish).
- Holmgren, J., Nilsson, M. & Olsson H. 2003. Estimation of tree height and stem volume on plots using airborne laser scanning. *Forest Science* 3, 419-428.
- Hyde, P., Nelson, R., Kimes, D., & Levine, E. 2007. Exploring LiDAR–RaDAR synergy—predicting aboveground biomass in a southwestern ponderosa pine forest using LiDAR, SAR and InSAR. *Remote Sensing of Environment* 1, 28-38.

Intergraph. 2006. Online source: <http://www.intergraph.com>. 2006, Case Study Digital Mapping Camera.

IPCC (Intergovernmental Panel on Climate Change) 2004. <http://www.ipcc.ch/index.htm>-2004.

Krantz, A. 2009. Mapping of clear-cuts in Swedish forest using satellite images acquired by the radar sensor ALOS PALSAR. Master thesis, SLU, Umea.

Lantmäteriverket. 2010. Online source: <http://www.lantmateriet.se>. 2010.

Leboeuf, A., Beaudoinb, A., Fourniera, R.A., Guindonb, L., Lutherc, J.E., & Lambertb, M.C. 2007. A shadow fraction method for mapping biomass of northern boreal black spruce forests using QuickBird imagery. *Remote Sensing of Environment* 4, 488-500.

Lu, D., Mauselb, P., Brondízioc, E., & Moran, E. 2004. Relationships between Forest stand parameters and Landsat TM spectral responses in the Brazilian Amazon Basin. *Forest Ecology and Management* 198, 149–167.

Magnusson, M & J.E.S Fransson. 2005. Estimation of forest stem volume using multispectral optical satellite and tree height data in combination. *Scandinavian Journal of Forest Research*, 20, 431-440.

Magnusson, M. 2006. Evaluation of Remote Sensing Techniques for Estimating of Forest variables at Stand Level, Doctoral Thesis, SLU,Umeå. ISSN 1652-6880.

Magnusson, M & J. E.S Fransson. 2007. Aerial photo interpretation using Z/I-DMC images for estimation of forest variables. *Scandinavian Journal of Forest Research* 22, 254-266.

Muukkonen. P & Heiskanen. J. 2005. Estimating biomass for boreal forests using ASTER satellite data combined with standwise forest inventory data. *Remote Sensing of Environment* 99, 434 – 447.

Næsset.E, 2008. Estimation of above- and below-ground biomass in across regions of the boreal forest zone using airborne laser. *Remote Sensing of Environment*, 6, 3079-3090.

Olsson. H, Egberth, M., Engberg, J., Fransson, E:S., Pahlen T.G., Hagner, O., Holmgren, J., Joyce, S., Magnusson, M., Nilsson, B., Nilsson, M., Olofsson, K., Reese, H., Wallerman, J. 2005. Current and emerging operational uses of remote sensing in Swedish forestry, *Proceedings of the Seventh Annual Forest inventory and Analysis Symposium*, pp 39-46.

Patenaude. G., Milne. R. & Dawson, T.P. 2005. Synthesis of remote sensing approaches for forest carbon estimation; reporting to the Kyoto Protocol. *Environmental Science and Policy* 8, 161-178.

- Petersson, H. 1999. Biomassfunktioner för trädfraktioner av tall, gran och björk i Sverige. Arbetsrapport 59. ISRN SLU-SRG-AR59SE, (in Swedish).
- Pohl, C. & Van Genderen, J.L. 1998. Multisensor image fusion in remote sensing: concepts, methods, and applications. *International Journal of Remote Sensing*, 19, 823-854.
- Popescu, S.C., Wynne, R.H. & Scriver, J.A. 2004. Fusion of small-footprint LiDAR and multispectral data to estimate plot-level volume and biomass in deciduous and pine forests in Virginia, USA. *Forest Science* 4, 551-565.
- Reese, H., Nilsson, M., Sandström, Per. & Olsson, H. 2002. Application using estimates of forest parameters derived from satellite and forest inventory data. *Computers and Electronics in Agriculture* 1-3, 37-55.
- Sandra, B. 1997. Estimating biomass and biomass change of tropical forest: a primer. FAO Forestry Paper-134.
- Wallerman, J. & Holmgren, J. 2007. Estimating field-plot data of forest stands using airborne laser scanning and SPOT HRG data. *Remote Sensing of Environment* 110, 501–508.
- Wulder, M.A., White, J.C., Fournier, R.A., Luther, J.E., & Magnussen, S. 2008. Spatially explicit large area biomass estimation: three approaches using forest inventory and remotely sensed imagery in a GIS. *Sensors* 8, 529-560.
- Zachary J.B & Randolph H.W. 2005. Estimating forest biomass using small footprint LIDAR data: an individual tree-based approach that incorporates training data. *ISPRS Journal of Photogrammetry and Remote Sensing* 6, 342-360.
- Zheng, D., Rademacher, J., Chena, J., Crowc, T., Breseea, M., Moined, J.L. & Ryua, S. 2004. Estimating aboveground biomass using Landsat 7 ETM+ data across a managed landscape in northern Wisconsin, USA. *Remote Sensing of Environment* 93, 402–411.